ISSN 1330-3651 (Print), ISSN 1848-6339 (Online)
https://doi.org/10.17559/TV-20220601114015
Original scientific paper

Hybrid Taguchi-GRA-CRITIC Optimization Method for Multi-Response Optimization of Micro-EDM Drilling Process Parameters

Ritesh Kumar SINGH, Sanjiv Kumar TIWARI*, Sharad Chandra SRIVASTAVA, Binay KUMAR

Abstract: In this study, an attempt is made to investigate how the operational parameters such as capacitance, voltage, feed rate, and rotating speed affect the material removal rate, tool wear, overcut, and taper angle for micro-EDM drilling of aluminium 6061 utilizing brass C360 electrode. A novel Taguchi-GRA-CRITIC hybrid optimization methodology is used to obtain the optimal combination of micro-EDM drilling process parameters. The experiment was designed using the Taguchi L18 orthogonal array, and responses were recorded for each experiment. Grey Relational Analysis (GRA) is applied to improve the multi-response of the planned experiment. The weighting values corresponding to various responses are determined using CRITIC (criterion importance through intercriteria correlation) analysis. The hybrid methodology determines the best combination of process parameters for different responses. ANOVA was used to discover the most critical parameters. Finally, confirmation experiments were conducted with optimal parameters to identify improvement in grey relational grade over the initial parameters. The study's findings indicate that, compared to the initial process parameter setting, the grey relational grade (GRG) increased by 92.36% with the optimal parameter setting.

Keywords: aluminium 6061; CRITIC; grey relational analysis; micro-EDM drilling; orthogonal array

1 INTRODUCTION

In the modern manufacturing era, the demand for miniaturized parts and micro-components is rapidly increasing due to their use in various domains, including electronics, biomedical, optical, energy, aerospace, automobile, and so on [1]. This has forced the manufacturing sectors to adopt new technologies to manufacture smaller, more intricate shapes. For manufacturing micro-components, various unconventional machining processes like electrical discharge machining (EDM), laser machining, and ultrasonic vibrations have emerged as viable options [2]. Micro-EDM (micro-electrical Discharge Machining) is an electro-thermal method used to produce microstructures, components, and micro tools [3].

Micro-EDM is an effective method for machining tough and brittle materials with greater precision, accuracy, and surface finish [1]. In the micro-EDM process, the tool does not directly contact the workpiece. An electrical spark causes the material removal. Furthermore, no heat-affected zone is produced during machining [2]. Micro-EDM is one of the most effective techniques for drilling micro-deep holes in metals [3]. These micro-deep holes are utilized for several applications, including diesel fuel injection nozzles, spinner holes, inkjet printer nozzles, turbine blade cooling channels, and drug delivery orifices [3].

However, there are some challenges and drawbacks to the micro-EDM process. One of the biggest challenges is the slow material removal rate. Additionally, during machining, the electrode itself undergoes erosion. Moreover, it is complex to machine holes with high aspect ratios [4]. Thus, appropriate process parameters are prime concerns to have the desired quality characteristics of the finished products. Most of the research in the literature mainly focuses on machining different metal alloys using various electrode materials, machining parameters and their impact on machining performance, methods for optimization of performance characteristics, application, working technology, and so on [1].

Aluminium alloy is extensively used in the aviation and automotive industries due to its superior mechanical characteristics like high strength-to-weight ratio, excellent machinability, high-temperature resistance, good surface finish at high cutting speed, and so on [5, 6]. On this basis, it is advantageous to study the micro-drilling by micro-EDM on Aluminium or its alloy.

Khan [7] reported his findings on Aluminium and mild steel material removal rate during EDM with copper and brass electrodes. To explore the effect of EDM process parameters on the surface quality of the Al 6063 SiCp metal matrix composite, Dvivedi et al. [8] created mathematical models utilizing response surface methods. The machinability of three Aluminium alloys, Al2219, Al7050, and Al7075, was investigated by Gatto et al. [9] to examine the electrode wear mechanism, dimensional and geometrical accuracy of the workpieces, and the surface finish. By altering electric current values, Arooj et al. [5] investigated the effect of surface morphology during the machining of Al 6061 T6 cylinders on die-sinking EDM machines. The white layer thickness, globule diameter, and inter-globule distance increase with increasing electric current, according to Arooj et al. [5]. Rao et al. [10] used the Taguchi technique to perform a parametric analysis of the wire EDM process on residual stresses in the machining of Aluminium alloy 2014 T6. Daneshmand et al. [11] investigated the effects of EDM parameters such as spark current intensity, frequency, and voltage on surface roughness when machining CK45 with copper tools and kerosene as the dielectric fluid. ANOVA and non-linear regression were used to further statistically analyze the experimental results. Finally, a mathematical model was developed to predict surface roughness. Dave et al. [12] investigated the influence of EDM input parameters, like current, pulse on time, and pulse off time, on drilling holes in AA 2024 alloy to reduce the difference between the actual and designed hole diameter. Further, Dave et al. [12] developed mathematical models using Response Surface Methodology (RSM), which were then optimized using the Genetic Algorithm (GA) to determine the input parameter settings that minimize the diameter difference.

Suresh Kumar et al. [13] reported an experimental study for multi-response optimization of EDM process parameters for machining Aluminium alloy (Al 6351-SiC-

B4C) hybrid metal matrix composite utilizing grey relational analysis. Jahan et al. [14] investigated the influence of various machining parameters on the machining properties of Aluminium alloy AA 2024 during micro-EDM. D'urso and Ravasio [3] examined the effect of MRR and electrode and workpiece materials' electrical and thermal properties on micro-EDM drilling performance. Rashid et al. [15] used the micro-EDM process to machine micro-holes on non-conductive Aluminium Nitride (AlN) ceramics by carefully selecting machining parameters and an assistive electrode. The results revealed that multi-layer coatings of silver and copper successfully machined micro-holes with a high aspect ratio with copper tungsten electrodes during powder-mixed micro-EDM of AlN ceramics. For milling Aluminium alloy Al5052 with EDM, Markopoulos et al. [16] examined the influence of pulse current and pulse on time.

From the above literature, it is evident that several operating parameters influence micro-EDM performance. Therefore, selecting optimal operating parameter combinations using a systematic method for arrangement and its statistical assessment is required to enhance the quality characteristics of micro-EDM. Traditionally, parametric optimization studies were carried out by varying a single parameter while holding other parameters fixed. But this process of parametric optimization is quite a tedious, time-consuming, and costly approach. Additionally, the number of experiments increases exponentially with the number of parameters studied.

Taguchi proposed orthogonal arrays (OA) to study the entire parameter space with only a few experiments [17, 18]. The effectiveness of the Taguchi method has extensively been in academia and industries for several decades [19]. However, most Taguchi applications are concerned with optimizing only one response. In contrast, most industrial problems involve multiple responses, frequently in conflict [20]. Multi-attribute decision-making (MADM) approaches are employed when more than one response must be analyzed. MADM selects the best responses from the existing options by evaluating several responses. Grey relational analysis (GRA) is one of the widely used MADM techniques to optimize multi-objective problems [21].

Grey relational analysis (GRA) is a part of Deng's grey system theory [22]. GRA can solve complex interrelationships between various variables and factors [20]. GRA solves MADM problems by merging the range of performance attribute values assessed for each alternative into a single value called grey relational grade (GRG) [21]. Several publications on multi-response optimization of process parameters utilizing the Taguchi-based Grey relational analysis approach can be found in the literature [19, 21, 23-26]. However, the biggest shortcoming of GRA is that it provides equal weight to each response during the optimization process, which could create some uncertainty as all responses do not affect the process [27]. In Criteria Importance Through Intercriteria Correlation (CRITIC) analysis, the factors are assigned according to their inner criteria correlations. It uses correlation analysis to determine the intensity of the contrast and the conflict between criteria in the structure of the decision-making problem [28]. Many CRITIC method applications can be found [28-30].

In this research, an attempt is made to investigate the effects of operating parameters, namely, capacitance, voltage, feed rate, and rotational speed, on the material removal rate, tool wear rate, overcut, and taper angle for micro-EDM drilling of Aluminium 6061 by using Brass C360 electrode. An optimal combination of micro-EDM drilling process parameters is determined by using a novel Hybrid Taguchi-GRA-CRITIC optimization methodology that overcomes the inherent GRA problem regarding the weight assignment to the responses. Taguchi L18 orthogonal array was used to design the experiment, and responses were recorded for each experiment. GRA is used to optimize the multi-response of the planned experiment. Criteria importance through intercriteria correlation (CRITIC) analysis is applied to determine the weighting values corresponding to various responses. Further, ANOVA is conducted to assess the contribution of different operating parameters to the multi-response of the micro-EDM drilling process. Finally, confirmation experiments are carried out using optimal parameters to find the improvement from the initial parameter settings.

The rest of the paper is structured as follows. Section 2 explores the theory behind the Taguchi technique, grey relational analysis (GRA), CRITIC analysis, and ANOVA. Section 3 discusses the proposed methodology for this study. Section 4 presents the experimental design used in this study. The experimental investigation, including experimental design and analysis, is covered in Section 5. Section 6 presents the empirical findings. Finally, sections 7 and 8 present the research's conclusions and future directions.

2 THEORETICAL BACKGROUNDS

2.1 Taguchi Method

The Taguchi method can be described as applying orthogonal arrays (OAs) for experimental design. It is one of the simplest and most frequently used process parameter optimization methods. The orthogonal array (OA) determines the near-optimal design parameter settings with the least possible experiments [31]. The selection of appropriate OA is based on total degrees of freedom. The degrees of freedom for the selected OA must be greater than, or at least equal to the sum of calculated degrees of freedom of the control factors and their interactions [18].

The Taguchi method employs the signal-to-noise (S/N) ratio as a statistical performance measure. The S/N ratio is a logarithmic function of the intended output that acts as an objective function for optimization. To measure the quality characteristics that deviated from the desired value, the experimental results were translated into S/N ratios using the Taguchi technique [32]. A higher S/N ratio was associated with better quality characteristics irrespective of the quality characteristic type. Three methods can calculate the S/N ratio [32]. These are:

a) Lower-the-better quality characteristics.

$$\eta_i = -10\log_{10}\left(\frac{1}{p}\sum_{j=1}^{p} y_{ij}^2\right) \tag{1}$$

b) Higher-the-better quality characteristics.

$$\eta_i = -10\log_{10}\left(\frac{1}{p}\sum_{j=1}^{p}\frac{1}{y_{ij}^2}\right) \tag{2}$$

c) Nominal-the-best quality characteristics.

$$\eta_i = 10\log_{10}\left(\frac{\bar{y}_i^2}{s_i^2}\right) \tag{3}$$

where

$$\bar{y}_i = \frac{y_1 + y_2 + y_3 + \ldots + y_p}{p}$$

$$s_i^2 = \frac{\left|\sum_{j=1}^{p}(y_{ij} - \bar{y})^2\right|}{p-1}$$

η_i - S/N ratio of the i^{th} experiment; y_{ij} - observed response of the i^{th} experiment for j^{th} trial; p - number of trails at the same parameter level; i = 1, 2, 3, …, n (n is the total runs of experiments to be conducted); j = 1, 2, 3, …, p (p is the total number of trails for each experiment run).

Eq. (1) is used when the quality characteristic must be minimized. Eq. (2) maximizes the required quality characteristic of interest. Eq. (3) minimizes the mean squared error around a given target value.

2.2 Grey Relational Analysis

GRA is based on the theory of grey relation space [33-35]. It measures the degree of correlation among factors based on their similarity or dissimilarity. GRA is characterized by its small data requirements and multifactor analysis [27]. In GRA, experimental data are of different quality characteristics with variable units. Therefore, normalizing the experimental data within the range of zero to one is required. Normalizing the data is known as pre-processing or grey relational generation [34]. Next, the Grey relational coefficient is calculated using normalized experimental data to indicate the correlation between the actual and desired experimental data. The grey relational grade (GRG) is then calculated using the mean of the grey relational coefficients associated with the selected responses [36]. The derived GRG determines the overall effectiveness of the multiple response processes. This approach converts multi-response optimization problems into a single-response optimization situation, with overall Grey relational grade as the objective function. The best parametric combination is then determined, yielding the highest GRG. The Taguchi approach can maximize the overall GRG by deciding the best factor combination. Finally, an experiment is conducted to confirm the optimal level of factors derived from the GRA for selected quality characteristics. The GRA theory and methods are explained in detail below.

Step 1: Depending on the type of quality characteristic, compute the S/N ratios for the corresponding responses using Eqs. (1) to (3) [19].

Step 2: Normalize the S/N ratios obtained in Step 1 from 0 to 1. The S/N ratio is normalized to eliminate the influence of different units and reduce variability [19]. The S/N ratio can be normalized using three approaches, as shown in Eqs. (4) to (6). Eq. (4) is used when the original sequence of the quality characteristics is lower-the-better. Similarly, Eqs. (5) and (6) are used for higher-the-better and nominal-the-best quality characteristics.

$$z_i(k) = \frac{\max\eta_i(k) - \eta_i(k)}{\max\eta_i(k) - \min\eta_i(k)} \tag{4}$$

$$z_i(k) = \frac{\eta_i(k) - \min\eta_i(k)}{\max\eta_i(k) - \min\eta_i(k)} \tag{5}$$

$$z_i(k) = \frac{\left|\eta_i(k) - \text{Target}\right| - \min\left|\eta_i(k) - \text{Target}\right|}{\max\left|\eta_i(k) - \text{Target}\right| - \min\left|\eta_i(k) - \text{Target}\right|} \tag{6}$$

where, $z_i(k)$ - normalized value of k^{th} response for i^{th} experiment obtained after the grey relational generation; $\eta_i(k)$ - S/N ratio of k^{th} response for i^{th} experiment; $\min\eta_i(k)$ - minimum value of $\eta_i(k)$ for k^{th} response; $\max\eta_i(k)$ - maximum value of $\eta_i(k)$ for k^{th} response; k = 1, 2, 3, …, m (m is the total number of responses).

Step 3: Compute the grey relational coefficient (GRC). After data pre-processing, a GRC is computed to illustrate the relationship between the actual and ideal normalized experimental outcomes [19]. The GRC is calculated as follows:

$$\xi_i(k) = \frac{\Delta_{\min} + \psi\Delta_{\max}}{\Delta_{0i}(k) + \psi\Delta_{\max}} \tag{7}$$

where, $\xi_i(k)$ - grey relational coefficient of k^{th} response for i^{th} experiment; $\Delta_{0i}(k)$ - quality loss function $= \left|z_0(k) - z_i(k)\right|$; $z_0(k)$ - reference sequence, which is equal to 1; $\Delta_{\min} = \min_{\forall j\in i}\min_{\forall k}\left|z_0(k) - z_i(k)\right|$; $\Delta_{\max} = \max_{\forall j\in i}\max_{\forall k}\left|z_0(k) - z_i(k)\right|$; ψ - identification coefficient; $\psi \in [0, 1]$, $\psi = 0.5$ is generally used.

Step 4: Compute the grey relational grade (GRG). The GRG is computed by taking the average of the calculated GRC. The GRG is calculated as follows [19]:

$$\gamma_i = \frac{1}{m}\sum_{k=1}^{m}\xi_i(k) \tag{8}$$

In real applications, however, the influence of each response on the system varies. Therefore, the modified equation for determining the grey relational grade is [27]:

$$\gamma_i = \sum_{k=1}^{m} w_k \cdot \xi_i(k) \tag{9}$$

where, γ_i - grey relational grade for i^{th} experiment; w_k - normalized weight for k^{th} response.

The grey relational grade in GRA depicts the relationship between sequences. The value of the grey relational grade is one if two sequences are identical. The grey relationship grade also shows how the comparability sequence influences the reference sequence. As a result, if a comparison sequence is more critical than others, its grey relational grade and reference sequence will be higher than those of other grey relational grades [27]. The associated weighting values w_k are derived from CRITIC analysis in this study.

Step 5: Determine the optimal factor combination and their level - the higher the grey relationship grade, the better the product quality [19]. Grey relational grade could determine the factor effect and the optimal level for a controllable factor. The influence of each factor (r = 1, 2, ..., t) is defined as:

$$\delta_r = \max \upsilon_{qr} - \min \upsilon_{qr} \tag{10}$$

where, δ_r - overall effect of r^{th} factor; υ_{qr} - average of grade value for q^{th} level of r^{th} factor.

The optimum level, q^* for the controllable factor r is determined as:

$$q^* = \max \upsilon_{qr} \tag{11}$$

Step 6: Lastly, the applicability of grey relational analysis is investigated [26]. After determining the optimal combination of factors and their levels by using GRG, the quality characteristics are predicted and validated using Eq. (12):

$$\gamma_{\text{predicted}} = \hat{\gamma} + \sum_{r=1}^{t} (\upsilon_{qr} - \hat{\gamma}) \tag{12}$$

2.3 CRITIC Analysis

In the multi-objective optimization process, various weight coefficient combinations might produce different solutions. It is, therefore, interesting to investigate how to develop better weight coefficient combinations. Subjective approaches have the limitation of involving the intervention of a decision-maker [37]. As a result, an objective approach without a decision-maker's subjective interference is needed, especially when there is no subjective preference among objectives [37]. Diakoulakiet al. [28] suggested the CRITIC approach as an objective weighing method for obtaining the objective weights of criteria in MCDM problems. The CRITIC method's basic idea is to determine each objective's weight based on contrast intensity and conflict measurement [38]. The standard deviation considers the contrast intensity of the criteria, and the correlation coefficient measures the conflict between them [39]. The standard deviation is used to characterize the variations between objective functions and quantify the contrast intensity of each objective. The larger the standard, the greater the contrast intensity, which entails the objective more important [40]. The correlation coefficient measures the conflict measurement between two compared objectives. If the correlation coefficient between the two objectives is more significant, the correlation is more substantial, and the conflict is lower [39].

The steps for the CRITIC method are given below:

Step 1: The original multiple-quality characteristic array [30]:

$$X = [X_{i(k)}]_{n\times m} = \begin{bmatrix} x_{1(1)} & x_{1(2)} & \cdots & x_{1(m)} \\ x_{2(1)} & x_{2(2)} & \cdots & x_{2(m)} \\ \vdots & \vdots & \ddots & \vdots \\ x_{n(1)} & x_{n(2)} & \cdots & x_{n(m)} \end{bmatrix} \tag{13}$$

where, $x_{i(k)}$ is the grey relational coefficient of each quality characteristic and n = 18, m = 4.

Step 2: Calculate the Correlation coefficient array [30]. The correlation coefficient array is estimated as follows:

$$\rho_{kl} = \left[\frac{\text{cov}(x_{i(k)}, x_{i(l)})}{\sigma(x_{i(k)}) \times \sigma(x_{i(l)})} \right] \tag{14}$$

where, ρ_{kl} - correlation coefficient of $x_{i(k)}$ and $x_{i(l)}$; where, k = 1, 2, 3, …, m and l = 1, 2, 3, …, m; $\text{cov}(x_{i(k)}, x_{i(l)})$ - covariance of sequences $x_{i(k)}$ and $x_{i(l)}$; $\sigma(x_{i(k)})$ - standard deviation of sequence $x_{i(k)}$; $\sigma(x_{i(l)})$ - standard deviation of sequence $x_{i(l)}$.

Step 3: Calculate the weight of the k^{th} criterion (w_k) as [30]:

$$w_k = \frac{c_k}{\sum_{l=1}^{m} c_l} \tag{15}$$

where,

$$c_k = \sigma_k \sum_{l=1}^{m} (1 - \rho_{kl}) \tag{16}$$

2.4 Analysis of Variance (ANOVA)

The ANOVA test investigates the most significant process parameters affecting quality characteristics. This is accomplished by subtracting the total variability of the S/N ratios from the mean of the S/N ratios. Fisher's test is used in ANOVA to examine whether a parameter significantly affects a quality characteristic. Fisher's ratio is the ratio of process parameter variance to error variance. This procedure compares the parameter's F-test value to the standard F table value (F0.05) at the 5% significance level. The process parameter is significant if the F-test value exceeds F0.05 [18].

3 HYBRID TAGUCHI-GRA-CRITIC METHODOLOGY

Fig. 1 shows the proposed hybrid Taguchi/GRA/CRITIC methodology for finding the best operating parameters combination for micro-EDM of AL 6061 using a Brass C360 electrode. The optimization

process determines the operational parameters and levels that affect the micro-EDM process. Then, using Taguchi's orthogonal arrays (OAs) for parametric design, experiments are designed and performed to determine the required quality characteristics. After recording the responses of the experimentations, the S/N ratio is calculated by using Eqs. (1) to (3) for each response, depending upon the quality characteristics.

These S/N ratios are further used as the raw data for grey relational analysis (GRA). In GRA, firstly, the S/N ratios of each response are normalized using Eqs. (4) to (6) to convert the responses into a single unit. Next, the grey relational coefficient (GRC) is computed using Eq. (7). Further, GRC calculates the corresponding weights for each response using CRITIC analysis by following Eqs. (13) to (16). These weights are additionally utilized for calculating the grey relational grade (GRG) using Eq. (9). Next, the optimal factor and its level combination are found using Eq. (11) to maximize grade values. After determining the optimal parameter settings, analysis of variance (ANOVA) is used to examine the most significant micro-EDM drilling parameters at a 95% confidence level. Finally, a confirmation test is performed to validate the designed experimentation.

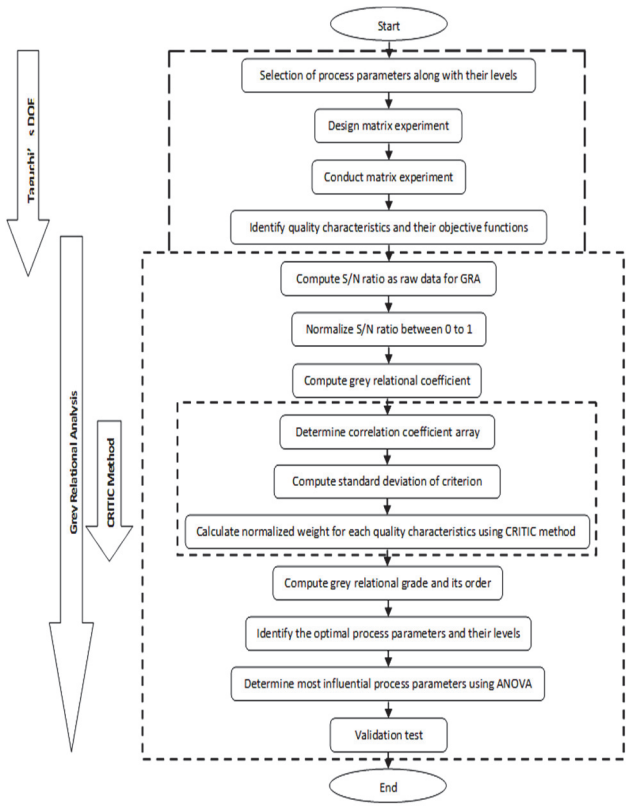

Figure 1 Hybrid Taguchi/GRA/CRITIC optimization methodology

4 EXPERIMENTAL SETUP

A Micro-EDM machine (Make: Mikrotools Pvt. Ltd., Singapore; Model: DT110) was utilized in this study to drill micro-holes on the workpiece using the Electrical Discharge Micro-Machining (EDMM) method, as shown in Fig. 2a. It is a three-axis CNC servo-controlled machine powered by an RC-type pulse generator. The maximum travel range of this machine is 200 mm on the *X*-axis, 100 mm on the *Y*-axis, and 100 mm on the *Z*-axis, with a resolution of 0.1 mm in all directions. It has a closed-loop control system that provides sub-micron accuracy. A variable-speed spindle drive allows the spindle to rotate up to 5000 rpm. Fig. 2b shows that the experimental setup comprises an electrode, a 0.5 mm diameter cylindrical Brass C360 rod securely mounted in the spindle. A fixture holds the workpiece in place. The workpiece material in this investigation is Al 6061, with 25 × 25 × 0.5 mm dimensions. Tab. 1 summarizes the corresponding physical properties of Al 6061 and Brass C360. The workpiece and the tool are immersed in EDM oil grade 3 during the machining process. An external flushing system with a pressure of 6 bar was employed to circulate the dielectric and provide appropriate flushing.

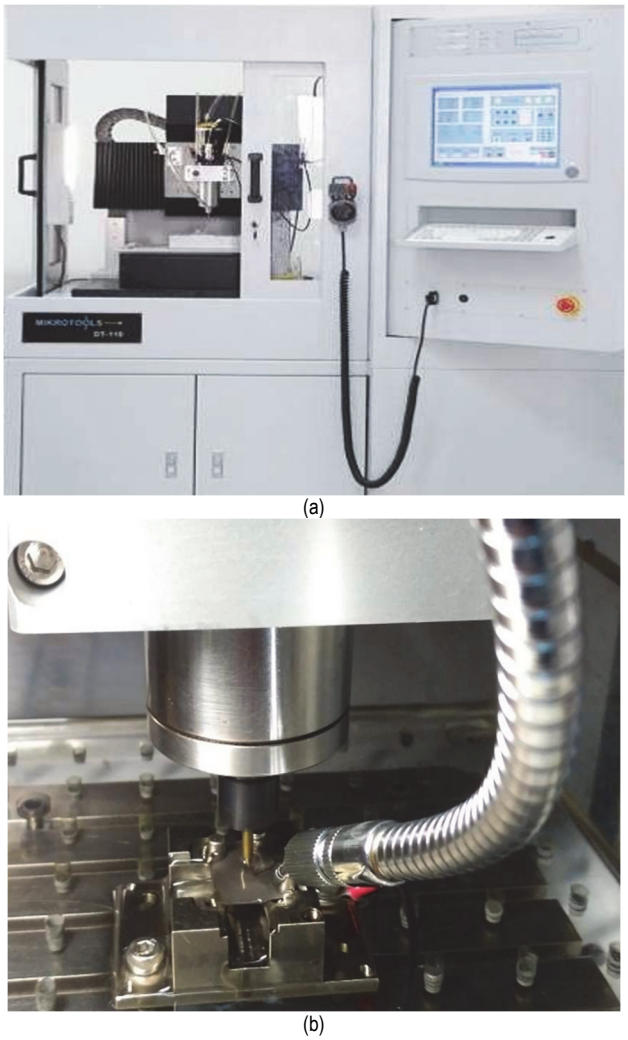

(a)

(b)

Figure 2 Photographic view of (a) Micro EDM machine (Make: Mikrotools Pvt. Ltd., Singapore; Model: DT110); and (b) Experimental setup

5 EXPERIMENTAL INVESTIGATION

5.1 Selection of Process Parameters

The Micro-EDM process's performance is affected by the voltage, capacitance, speed, feed rate, dielectric, flushing pressure, polarity, and other variables. Among these, voltage (*V*), capacitance (*C*), electrode rotational speed (*N*), and feed rate (*F*) are the primary factors that affect the performance of the Micro-EDM process. As a result, these four parameters are used as inputs in the experimental design. Tab. 2 shows the selected process parameters, along with their ranges.

Table 1 Physical properties of Al 6061 and Brass C360

Physical properties	Al 6061	Brass C360
Density (ρ)	2700 kg/m^3	8700 kg/m^3
Young's modulus (E)	68.9 × 10^3 MPa	251 MPa
Tensile strength (σ_t)	310 MPa	270 MPa
Elongation (ε) at break	12-25%	25%
Poisson's ratio (ν)	0.33	0.31
Melting temperature (T_m)	585 °C	885-900 °C
Thermal conductivity (k)	151-202 W/(m·K)	115 W/(m·K)

Table 2 Input parameters and their levels

Notation	Parameters	Range	Level		
			1	2	3
C	Capacitance / pF	4-5	4	5	-
V	Voltage / volts	90-130	90	110	130
F	Feed rate / µm/s	0.3-0.9	0.3	0.6	0.9
N	Rotation Speed / rpm	1000-2000	1000	1500	2000

5.2 Design Matrix Experimental

In this study, interactions of input process parameters have not been considered. Therefore, with one parameter (capacitance) having two levels and other parameters (voltage, electrode rotational speed, and feed rate) having three levels, L_{18} OA is selected with 18 experimental runs and four columns. The experimental design for conducting the experiments is shown in Tab. 3.

5.3 Conduct Matrix Experiment and Identify Quality Characteristics

The experiments were conducted once the parameters were assigned to the experimental array. Material removal rate (MRR), tool wear rate (TWR), overcut (OC), and taper angle (TA) were selected as output responses to evaluate the performance characteristics of the process. The physical quantities required to calculate output responses were found using different measuring devices. The digital vernier caliper measured the thickness of the workpiece. The digital multi-meter performed a conductivity test. An optical and digital microscope determined the analysis and size of the holes. The output responses were determined by using the following equations:

$$MRR = \frac{\pi \cdot h \cdot (D_{\text{top}}^2 + D_{\text{top}} \cdot D_{\text{bottom}} + D_{\text{bottom}}^2)}{12t} \tag{17}$$

$$TWR = \frac{\pi \cdot h_1 \cdot d^2}{4t} \tag{18}$$

$$OC = \frac{D_{\text{top}} - d}{2} \tag{19}$$

$$TA = \tan^{-1}\left(\frac{D_{\text{top}} - D_{\text{bottom}}}{2h}\right) \tag{20}$$

where, MMR - material removal rate in mm^3/min; TWR - tool wear rate in mm^3/min; OC - overcut in mm; TA - taper angle in degree; h - thickness of the workpiece in mm; D_{top} and D_{bottom} - top and bottom diameters of the hole measured by an optical measuring microscope at a magnification of 100X in mm; t - machining time recorded by the EDM system in min; h_1 - height equal to the measured tool wear = initial tool height - final tool height in mm; d - diameter of the tool in mm.

6 ANALYSIS AND DISCUSSION OF EXPERIMENTAL RESULTS

6.1 Experimental Results of the Taguchi Method

This study conducted three trials with the same parameters, measuring MRR, TWR, OC, and TA responses in each trial. In addition, the average was calculated for each trial and response. Tab. 3 shows the mean values of these output responses based on Taguchi's experimental design. Subsequently, the S/N ratio is calculated by using MINITAB® 15 for each response using Eqs. (1) to (3) based on the type of quality characteristics. Tab. 3 shows the estimated S/N ratio values for each response. In this study, MRR is taken as higher-the-better quality characteristics, and TWR, OC, and TA are expressed as lower-the-better-quality characteristics. The effect of S/N ratios for the individual process parameters on the MRR, TWR, OC, and TA is summarized in Fig. 3.

From Fig. 3, it can be concluded that capacitance has the most dominant effect on all the quality characteristics. The discharge energy between the electrode and the workpiece increases as the capacitance value increases (from 4pF to 5pF), increasing the spark size. This significantly increases the amount of material removed per spark (see Fig. 3a). In addition, higher discharge energy forms more gas bubbles in the spark gap, and debris will also increase. So, when the next spark is generated, that spark cannot reach the workpiece due to the debris in the spark gap. So, no material removal takes place and the time required to machine increases, which means more sparks are needed to remove the same amount of material due to the unstable machining. Therefore, more electrode wear occurs, as shown in Fig. 3b.

The difference between the tool diameter and the hole diameter is known as overcut (OC). The debris produced following the spark is the primary cause of overcutting. The spark occurs sideways due to debris passage in the spark gap. Due to side spark material being removed from the boundary, increasing the diameter of the hole being machined and causing overcut. This effect is more dominant when the discharge energy is higher because more side spark occurs with more discharge energy. This phenomenon leads to higher material removal, thereby increasing the debris concentration in the spark gap, eventually leading to overcut, as shown in Fig. 3c. Overcut increases when the capacitance and voltage increase, which can be easily related. Both factors cause the discharge energy to increase, increasing the overcut.

The tapered hole occurred due to the difference in the hole's top diameter and bottom diameter. The hole tapering occurs during the machining process when secondary discharges increase significantly due to incomplete removal of debris, leading to unstable spark conditions. The debris flows in an upward direction after removal. Therefore, a side spark occurs near the hole's top side, increasing its diameter. As shown in Fig. 3d, the taper angle increases with capacitance and voltage because these parameters are directly linked to the discharge energy, which leads to an increased side spark due to increased debris concentration.

Table 3 Experimental assignments, results, and S/N ratio

Exp. No.	Input Parameters				Responses				S/N Ratio / dB			
	C	*V*	*F*	*N*	*MRR*	*TWR*	*OC*	*TA*	*MRR*	*TWR*	*OC*	*TA*
1	4	90	0.3	1000	2.91×10^{-6}	4.26×10^{-4}	7.51×10^{-3}	8.25×10^{-2}	–110.74	67.41	42.49	21.67
2	4	90	0.6	1500	3.81×10^{-6}	6.72×10^{-4}	7.91×10^{-3}	19.23×10^{-2}	–108.38	63.45	42.04	14.32
3	4	90	0.9	2000	3.31×10^{-6}	13.02×10^{-4}	18.22×10^{-3}	23.94×10^{-2}	–109.61	57.71	34.79	12.42
4	4	110	0.3	1000	3.34×10^{-6}	4.89×10^{-4}	15.32×10^{-3}	45.71×10^{-2}	–109.53	66.21	36.29	6.80
5	4	110	0.6	1500	4.43×10^{-6}	3.09×10^{-4}	15.02×10^{-3}	46.47×10^{-2}	–107.07	70.20	36.47	6.66
6	4	110	0.9	2000	5.12×10^{-6}	8.87×10^{-4}	15.58×10^{-3}	46.73×10^{-2}	–105.81	61.04	36.15	6.61
7	4	130	0.3	1500	4.49×10^{-6}	8.01×10^{-4}	15.02×10^{-3}	40.11×10^{-2}	–106.96	61.93	36.47	7.94
8	4	130	0.6	2000	5.23×10^{-6}	4.5×10^{-4}	13.80×10^{-3}	23.94×10^{-2}	–105.63	66.94	37.20	12.42
9	4	130	0.9	1000	5.84×10^{-6}	9.85×10^{-4}	23.06×10^{-3}	15.79×10^{-2}	–104.67	60.13	32.74	16.03
10	5	90	0.3	2000	29.92×10^{-6}	36.65×10^{-4}	27.75×10^{-3}	72.95×10^{-2}	–90.48	48.72	31.13	2.74
11	5	90	0.6	1000	21.44×10^{-6}	25.96×10^{-4}	27.80×10^{-3}	82.76×10^{-2}	–93.38	51.71	31.12	1.64
12	5	90	0.9	1500	23.99×10^{-6}	28.22×10^{-4}	26.10×10^{-3}	97.61×10^{-2}	–92.40	50.99	31.67	0.21
13	5	110	0.3	1500	24.99×10^{-6}	30.92×10^{-4}	26.13×10^{-3}	116.62×10^{-2}	–92.05	50.20	31.66	–1.34
14	5	110	0.6	2000	31.29×10^{-6}	45.11×10^{-4}	26.09×10^{-3}	77.04×10^{-2}	–90.09	46.91	31.67	2.27
15	5	110	0.9	1000	20.91×10^{-6}	34.83×10^{-4}	25.69×10^{-3}	131.76×10^{-2}	–93.59	49.16	31.80	–2.40
16	5	130	0.3	2000	25.41×10^{-6}	37.69×10^{-4}	27.69×10^{-3}	129.20×10^{-2}	–91.90	48.48	31.15	–2.23
17	5	130	0.6	1000	23.29×10^{-6}	38.28×10^{-4}	29.47×10^{-3}	158.03×10^{-2}	–92.66	48.34	30.61	–3.97
18	5	130	0.9	1500	24.22×10^{-6}	49.55×10^{-4}	25.06×10^{-3}	584.43×10^{-2}	–92.32	46.10	32.02	–15.33

Table 4 Normalized S/N ratio, quality loss function, and grey relational co-efficient for all experimental runs

Exp. No.	Normalized S/N ratio				Quality loss function				Grey relational co-efficient			
	MRR	*TWR*	*OC*	*TA*	*MRR*	*TWR*	*OC*	*TA*	*MRR*	*TWR*	*OC*	*TA*
1	0.0000	0.1157	0.0000	0.0000	1.0000	0.8843	1.0000	1.0000	0.3333	0.3612	0.3333	0.3333
2	0.1141	0.2800	0.0380	0.1986	0.8859	0.7200	0.9620	0.8014	0.3608	0.4098	0.3420	0.3842
3	0.0547	0.5183	0.6483	0.2500	0.9453	0.4817	0.3517	0.7500	0.3460	0.5093	0.5870	0.4000
4	0.0585	0.1654	0.5215	0.4019	0.9415	0.8346	0.4785	0.5981	0.3469	0.3747	0.5110	0.4553
5	0.1774	0.0000	0.5070	0.4057	0.8226	1.0000	0.4930	0.5943	0.3781	0.3333	0.5035	0.4569
6	0.2388	0.3800	0.5338	0.4070	0.7612	0.6200	0.4662	0.5930	0.3964	0.4464	0.5175	0.4575
7	0.1831	0.3433	0.5070	0.3712	0.8169	0.6567	0.4930	0.6288	0.3797	0.4323	0.5035	0.4429
8	0.2473	0.1355	0.4450	0.2500	0.7527	0.8645	0.5550	0.7500	0.3991	0.3664	0.4740	0.4000
9	0.2938	0.4178	0.8206	0.1524	0.7062	0.5822	0.1794	0.8476	0.4145	0.4620	0.7359	0.3710
10	0.9812	0.8913	0.9560	0.5116	0.0188	0.1087	0.0440	0.4884	0.9638	0.8214	0.9191	0.5058
11	0.8409	0.7670	0.9573	0.5412	0.1591	0.2330	0.0427	0.4588	0.7587	0.6822	0.9214	0.5215
12	0.8882	0.7971	0.9112	0.5799	0.1118	0.2029	0.0888	0.4201	0.8172	0.7114	0.8491	0.5434
13	0.9054	0.8301	0.9120	0.6217	0.0946	0.1699	0.0880	0.3783	0.8408	0.7463	0.8504	0.5693
14	1.0000	0.9662	0.9109	0.5244	0.0000	0.0338	0.0891	0.4756	1.0000	0.9366	0.8487	0.5125
15	0.8305	0.8730	0.8996	0.6503	0.1695	0.1270	0.1004	0.3497	0.7468	0.7974	0.8328	0.5885
16	0.9124	0.9014	0.9544	0.6457	0.0876	0.0986	0.0456	0.3543	0.8509	0.8353	0.9165	0.5853
17	0.8757	0.9070	1.0000	0.6930	0.1243	0.0930	0.0000	0.3070	0.8010	0.8432	1.0000	0.6196
18	0.8922	1.0000	0.8814	1.0000	0.1078	0.0000	0.1186	0.0000	0.8227	1.0000	0.8083	1.0000

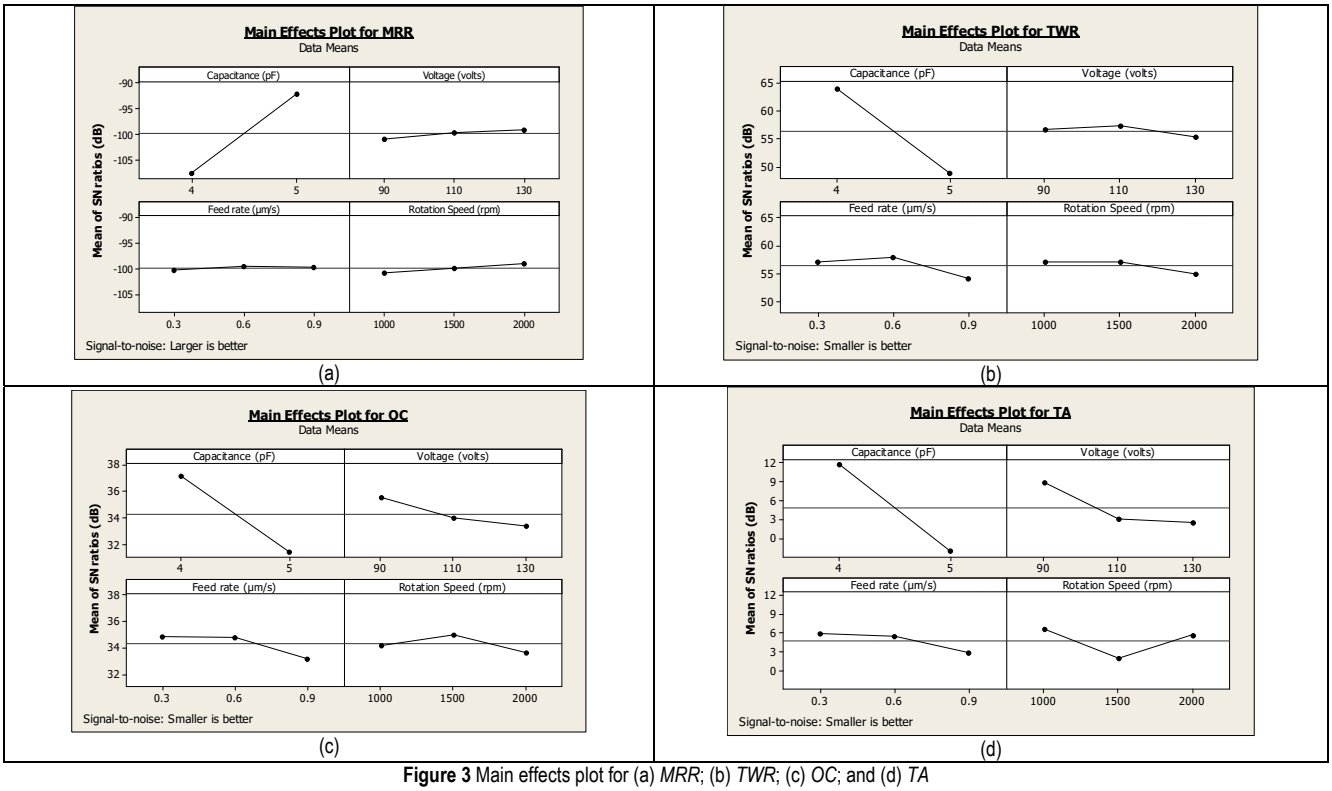

Figure 3 Main effects plot for (a) *MRR*; (b) *TWR*; (c) *OC*; and (d) *TA*

6.2 Multi-Response Optimization Using GRA and CRITIC Analysis

This section determines the optimal parameter combinations of the micro-EDM drilling process based on GRA coupled with CRITIC analysis.

Step 1: Calculate the S/N ratios. Tab. 3 shows the corresponding S/N ratio values for each response based on the type of quality characteristics.

Step 2: Normalize the S/N ratios. The S/N ratio can be normalized using Eqs. (4) to (6). The results are summarized in Tab. 4. For instance, using Eq. (5), the normalized S/N ratio of MRR for experiment 1 can be calculated as follows:

$$z_1(1) = \frac{-110.74 - 110.74}{-99.09 - 110.74} = 0.00$$

Further, using the Eq. $|z_0(k) - z_i(k)|$, quality loss functions were computed (depicted in Tab. 4) to identify the variation of the responses from the required value.

$$\Delta_{01}(1) = |1 - 0| = 1$$

Step 3: Grey relational coefficient (GRC) was computed using Eq. (7). The resultant values of GRC for each response are expressed in Tab. 4.

$$\xi_1(1) = \frac{0 + (0.5 \times 1)}{1 + (0.5 \times 1)} = 0.3333$$

Step 4: The next step was to apply CRITIC analysis to calculate the weights for each response to reflect its relative importance in GRA. The array of GRC (calculated in Step 3) was used to calculate the correlation coefficient and standard deviation using Eq. (14). The correlation coefficient and standard deviation values for each quality characteristic are portrayed in Tabs. 5 and 6, respectively. Subsequently, the corresponding weights for each quality characteristic were calculated using Eq. (15). The same is shown in Tab. 6. These weights were further used for calculating the GRG.

Table 5 Correlation coefficient of quality characteristics

	MRR	*TWR*	*OC*	*TA*
MRR	1.0000	0.9396	0.8915	0.6170
TWR	0.9396	1.0000	0.8667	0.7707
OC	0.8915	0.8667	1.0000	0.5742
TA	0.6170	0.7707	0.5742	1.0000

Table 6 Standard deviation and overall weight of quality characteristics

	MRR	TWR	OC	TA
STD. DEV.	0.2505	0.2250	0.2173	0.1480
W_k	0.2598	0.1789	0.2726	0.2887

Step 5: After determining the GRC for each quality characteristic (Tab. 4) and their corresponding weights (Tab. 6), the GRG corresponding to each experimental run was calculated based on Eq. (9).

$$\gamma_1 = 0.3333 \times 0.2598 + 0.3612 \times 0.1789 + 0.3333 \times 0.2726 + 0.3333 \times 0.2887 = 0.3383$$

Tab. 7 summarizes the GRG values obtained and their order. As a result, the optimization design was done for a single grey relational grade rather than having many performance criteria. Experiment No. 17's micro-EDM drilling parameters setting has the highest grey relation grade, as shown in Tab. 7 and Fig. 4. Thus, among the 18 experiments, the 17th provides the best multi-performance characteristics.

Table 7 Grey relational grade and its order for all experimental runs

Exp. No.	Grey relational Grade	Order
1	0.3383	18
2	0.3712	17
3	0.4565	11
4	0.4279	14
5	0.4270	15
6	0.4560	12
7	0.4411	13
8	0.4139	16
9	0.4981	10
10	0.7940	4
11	0.7209	9
12	0.7280	8
13	0.7481	6
14	0.8067	2
15	0.7336	7
16	0.7893	5
17	0.8104	1
18	0.8017	3

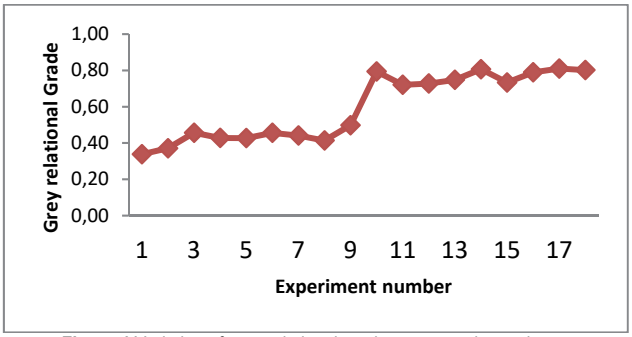

Figure 4 Variation of grey relational grade w.r.t experimental runs

Step 6: Next, the optimal factor and its level combination were determined by considering the maximization of grade values using Eq. (11). The resultants of the average grade value for q^{th} level of r^{th} factor are depicted in Tab. 8.

Table 8 Response table for grey relational grade

Factors	1	2	3	Max. - Min.
C	0.4256	**0.7703**		0.3447
V	0.5681	0.5999	**0.6258**	0.0577
F	0.5898	0.5917	**0.6123**	0.0225
N	0.5882	0.5862	**0.6194**	0.0332

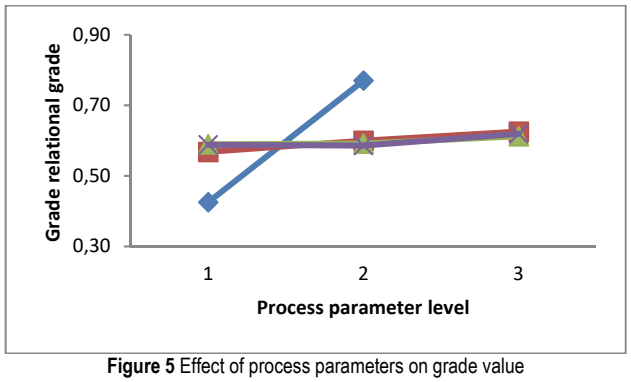

Figure 5 Effect of process parameters on grade value

From Fig. 5, it can be concluded that the optimal process parameters conditions are $C_2V_3F_3N_3$, i.e., the capacitance of 5 pF, the voltage of 130 volts, feed rate of 0.9 μm/s, and the rotational speed of 2000 rpm.

6.3 Analysis of Variance

The ANOVA method is used to investigate the most critical micro-EDM drilling parameters. Tab. 9 exhibits the ANOVA results. Tab. 9 shows that capacitance (*C*) and voltage (*V*) are essential parameters affecting quality characteristics, with *P*-values less than 0.05.

Fig. 6 also illustrates the percentage contribution of each process parameter to the total variation, illustrating the degree to which they influence the micro-EDM drilling process. The percentage contribution of capacitance (92.39%) has the most significant influence on overall variance, followed by voltage (1.54%), feed rate (0.25%), and rotation speed (0.11%).

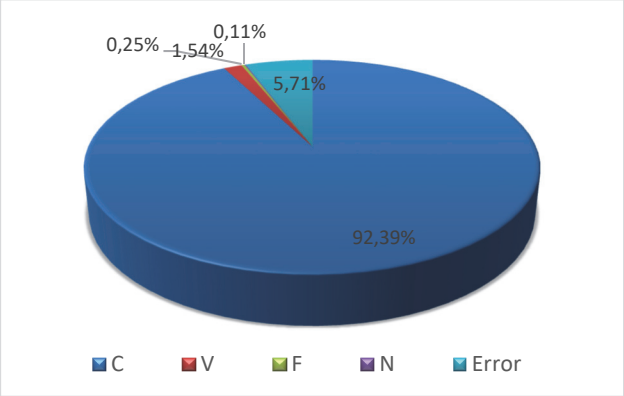

Figure 6 Percentage contributions of parameters in the grey relational grade

Table 9 ANOVA summary

Source	DF	SS	MS	*F*-value	*P*-value	% Contribution
C	1	121.465	121.465	276.31	0.000	92.39
V	2	2.899	1.450	4.41	0.042	1.54
F	2	1.202	0.601	1.37	0.299	0.25
N	2	1.025	0.512	1.17	0.351	0.11
Error	10	4.396	0.440			5.71
Total	17	130.987				100

6.4 Confirmation Test

The final step in GRA is to anticipate and validate performance characteristics using the optimal process parameter level combination once the optimal level of the variables has been found.

Table 10 Results of the confirmation test

Response	Initial parameters combination	Optimal parameters combination	
		Prediction	Experiment
Level	$C_1V_2F_2N_2$	$C_2V_3F_3N_3$	$C_2V_3F_3N_3$
MRR	4.43×10^{-6}		24.29×10^{-6}
TWR	3.09×10^{-4}		$43.28 \times 10^{-}$
OC	15.02×10^{-3}		26.47×10^{-3}
TA	46.47×10^{-2}		147.03×10^{-2}
GRG	0.4270	0.8341	0.8214
Improvement in *GRG*		95.34%	92.36%
Error	1.52%		

Tab. 10 presents the results of the confirmation trials utilizing the optimal process parameters for *MRR*, *TWR*, *OC*, and *TA*. Furthermore, the confirmation test exhibits a good agreement between the predicted and experimental value, as the error was found to be 1.52% only. Additionally, the improvement in the *GRG* value was 92.36%. This improvement in the experimental results over the initial parameter design confirms the validation of the proposed hybrid Taguchi-GRA-CRITIC methodology to enhance the micro-EDM drilling process's performance.

7 CONCLUSION

A hybrid Taguchi-GRA-CRITIC methodology investigated the optimal parameter combination for the micro-EDM drilling process. The drilling was done on Al 6061 sheet with the help of the Brass C360 electrode. The various input process parameters taken into consideration were capacitance (*C*), voltage (*V*), feed rate (*F*), and electrode rotation speed (*N*). Using L18 Taguchi orthogonal array (*OA*), various experiments were conducted in series, considering all factors at three levels except capacitance which was selected at two levels. The material removal rate (*MRR*), tool wear rate (*TWR*), overcut (*OC*), and taper angle (*TA*) for each experimental run were then calculated.

Furthermore, grey relational analysis and CRITIC analysis optimized the micro-EDM drilling process. The CRITIC analysis was performed to determine the weightage of each performance characteristic while using grey relational analysis. The optimal combination of the micro-EDM drilling process was found to be capacitance at level 2 (5 pF), voltage at level 3 (130 volts), feed rate at level 3 (0.9 μm/s), and rotational speed at level 3 (2000 rpm); i.e., $C_2V_3F_3N_3$. From ANOVA results, capacitance (*C*) and voltage (*V*) were the most significant parameters affecting quality characteristics. Additionally, the percentage contribution of capacitance (51.19%) has the most prominent effect on total variance, followed by voltage (1.58%), feed rate (0.83%), and rotation speed (0.31%). With the optimal parameters setting, an increase of 92.36% in the grey relational grade (*GRG*) value was found against the initial process parameters setting.

8 FUTURE SCOPE

This research emphasizes finding the effect of input parameters and optimizing the output parameters with the help of Micro-EDM on AL 6061 alloy using Brass C360 as the electrode. As a result, some suggestions for improving the process are mentioned below, improving the process's efficiency even more.

- Here capacitance is only taken at two levels to study the effect. Further, it can be taken at three levels.
- Proper flow of dielectric is essential for stable machining conditions; therefore, proper investigation is required into which dielectric pressure can be taken as an input parameter.

- The use of dielectric additives can enhance the machining conditions and make the spark stable.
- Using different shape electrodes has other effects which need to be further studied. For example, spiral and square-shaped tools can be used.
- Electrode plays an essential part in the machining process. Therefore, coating on brass can enhance its property even further.

9 REFERENCES

[1] Boral, S., Sidhu, S. S., Chatterjee, P., Chakraborty, S., & Gugaliya, A. (2019). Multi-response Optimization of Micro-EDM Processes: A State-of-the-Art Review. *Micro-electrical Discharge Machining Processes*, 293-310. https://doi.org/10.1007/978-981-13-3074-2_13

[2] Abidi, M. H., Al-Ahmari, A. M., Umer, U., & Rasheed, M. S. (2018). Multi-objective optimization of micro-electrical discharge machining of nickel-titanium-based shape memory alloy using MOGA-II. *Measurement*, *125*, 336-349. https://doi.org/10.1016/j.measurement.2018.04.096

[3] D'urso, G. & Ravasio, C. (2017). Material-Technology Index to evaluate micro-EDM drilling process. *Journal of Manufacturing Processes*, *26*, 13-21. https://doi.org/10.1016/j.jmapro.2017.01.003

[4] Fu, Y., Miyamoto, T., Natsu, W., Zhao, W., & Yu, Z. (2016). Study on influence of electrode material on hole drilling in micro-EDM. *Procedia CIRP*, *42*, 516-520. https://doi.org/10.1016/j.procir.2016.02.243

[5] Arooj, S., Shah, M., Sadiq, S., Jaffery, S. H. I., & Khushnood, S. (2014). Effect of current in the EDM machining of aluminum 6061 T6 and its effect on the surface morphology. *Arabian Journal for Science and Engineering*, *39*(5), 4187-4199. https://doi.org/10.1007/s13369-014-1020-z

[6] Jahan, M. P., Kakavand, P., Kwang, E. L. M., Rahman, M., & Wong, Y. S. (2015). An experimental investigation into the micro-electro-discharge machining behaviour of aluminium alloy (AA 2024). *The International Journal of Advanced Manufacturing Technology*, *78*(5), 1127-1139. https://doi.org/10.1007/s00170-014-6712-8

[7] Khan, A. A. (2008). Electrode wear and material removal rate during EDM of aluminum and mild steel using copper and brass electrodes. *The International Journal of Advanced Manufacturing Technology*, *39*(5), 482-487. https://doi.org/10.1007/s00170-007-1241-3

[8] Dvivedi, A., Kumar, P., & Singh, I. (2010). Effect of EDM process parameters on surface quality of Al 6063 SiCp metal matrix composite. *International Journal of Materials and Product Technology*, *39*(3-4), 357-377. https://doi.org/10.1504/IJMPT.2010.035843

[9] Gatto, A., Bassoli, E., & Iuliano, L. (2011). Performance Optimization in Machining of Aluminium Alloys for Moulds Production: HSM and EDM. *Aluminium Alloys, Theory and Applications*, 355-376. https://doi.org/10.5772/14847

[10] Rao, P. S., Ramji, K., & Satyanarayana, B. (2016). Effect of wire EDM conditions on generation of residual stresses in machiningof aluminum 2014 T6 alloy. *Alexandria Engineering Journal*, *55*(2), 1077-1084. https://doi.org/10.1016/j.aej.2016.03.014

[11] Daneshmand, S., Neyestanak, A. A. L., & Monfared, V. (2016). Modeling and investigating the effect of input parameters on surface roughness in electrical discharge machining of CK45. *Tehnički Vjesnik - Technical Gazette*, *23*(3), 725-730. https://doi.org/10.17559/TV-20141024224809

[12] Dave, S., Vora, J. J., Thakkar, N., Singh, A., Srivastava, S., Gadhvi, B., ... & Kumar, A. (2016). Optimization of EDM drilling parameters for Aluminum 2024 alloy using Response Surface Methodology and Genetic Algorithm. In *Key Engineering Materials*, *706*, 3-8. https://doi.org/10.4028/www.scientific.net/KEM.706.3

[13] Suresh Kumar, S., Uthayakumar, M., Thirumalai Kumaran, S., Parameswaran, P., & Mohandas, E. (2014). Electrical discharge machining of Al (6351)-5% SiC-10% B4C hybrid composite: a grey relational approach. *Modeling and Simulation in Engineering*, *2014*, 1-7. https://doi.org/10.1155/2014/426718

[14] Jahan, M. P., Kakavand, P., Kwang, E. L. M., Rahman, M., & Wong, Y. S. (2015). An experimental investigation into the micro-electro-discharge machining behaviour of aluminium alloy (AA 2024). *The International Journal of Advanced Manufacturing Technology*, *78*(5), 1127-1139. https://doi.org/10.1007/s00170-014-6712-8

[15] Rashid, A., Bilal, A., Liu, C., Jahan, M. P., Talamona, D., & Perveen, A. (2019). Effect of conductive coatings on micro-electro-discharge machinability of aluminum nitride ceramic using on-machine-fabricated microelectrodes. *Materials*, *12*(20), 3316. https://doi.org/10.3390%2Fma12203316

[16] Markopoulos, A. P., Papazoglou, E. L., & Karmiris-Obratański, P. (2020). Experimental study on the influence of machining conditions on the quality of electrical discharge machined surfaces of aluminum alloy Al5052. *Machines*, *8*(1), 12. https://doi.org/10.3390/machines8010012

[17] Payal, H., Bharti, P. S., Maheshwari, S., & Agarwal, D. (2020). Machining characteristics and parametric optimisation of Inconel 825 during electric discharge machining. *Tehnički vjesnik*, *27*(3), 761-772. https://doi.org/10.17559/TV-20190214135509

[18] Tiwari, S. K., Singh, R. K., & Srivastava, S. C. (2016). Optimisation of green sand casting process parameters for enhancing quality of mild steel castings. *International Journal of Productivity and Quality Management*, *17*(2), 127-141. https://dx.doi.org/10.1504/IJPQM.2016.074446

[19] Raza, Z. A., Ahmad, N., & Kamal, S. (2014). Multi-response optimization of rhamnolipid production using grey rational analysis in Taguchi method. *Biotechnology Reports*, *3*, 86-94. https://doi.org/10.1016/j.btre.2014.06.007

[20] Kuo, Y., Yang, T., & Huang, G. W. (2008). The use of a grey-based Taguchi method for optimizing multi-response simulation problems. *Engineering Optimization*, *40*(6), 517-528. https://doi.org/10.1080/03052150701857645

[21] Pervez, M., Shafiq, F., Sarwar, Z., Jilani, M. M., & Cai, Y. (2018). Multi-response optimization of resin finishing by using a Taguchi-based grey relational analysis. *Materials*, *11*(3), 426. https://doi.org/10.3390/ma11030426

[22] Ju-Long, D. (1982). Control problems of grey systems. *Systems & control letters*, *1*(5), 288-294. https://doi.org/10.1016/S0167-6911(82)80025-X

[23] Ay, M., Çaydaş, U., & Hasçalık, A. (2013). Optimization of micro-EDM drilling of Inconel 718 superalloy. *The International Journal of Advanced Manufacturing Technology*, *66*(5), 1015-1023. https://doi.org/10.1007/s00170-012-4385-8

[24] Puh, F., Jurkovic, Z., Perinic, M., Brezocnik, M., & Buljan, S. (2016). Optimization of machining parameters for turning operation with multiple quality characteristics using Grey relational analysis. *Tehnički vjesnik*, *23*(2), 377-382. https://doi.org/10.17559/TV-20150526131717

[25] Mavi, A. (2020). Evaluation of cutting parameters by determination of the grey correlation analysis methods of the effects on the cutting force and surface roughness of duplex stainless steels (2205). *Tehnički vjesnik*, *27*(1), 270-275. https://doi.org/10.17559/TV-20181220075328

[26] Achuthamenon Sylajakumari, P., Ramakrishnasamy, R., & Palaniappan, G. (2018). Taguchi grey relational analysis for

multi-response optimization of wear in co-continuous composite. *Materials*, *11*(9), 1743. https://doi.org/10.3390/ma11091743

[27] Mehat, N. M., Kamaruddin, S., Othman, A. R., Mehat, N. M., Kamaruddin, S., & Othman, A. R. (2014). Hybrid integration of Taguchi parametric design, grey relational analysis, and principal component analysis optimization for plastic gear production. *Chinese Journal of Engineering*, *351206*(1-11), 2014. https://doi.org/10.3390/ma15196623

[28] Diakoulaki, D., Mavrotas, G., & Papayannakis, L. (1995). Determining objective weights in multiple criteria problems: The critic method. *Computers & Operations Research*, *22*(7), 763-770. https://doi.org/10.1016/0305-0548(94)00059-H

[29] Madic, M., & Radovanovic, M. (2015). Ranking of some most commonly used nontraditional machining processes using ROV and CRITIC methods. *UPB Sci. Bull., Series D*, *77*(2), 193-204.

[30] Adali, E. A. (2017). CRITIC and MAUT methods for the contract manufacturer selection problem. *European Journal of Multidisciplinary Studies*, *2*(5), 93-101.

[31] Ross, P. J. (1988). *Taguchi Technique for Quality Engineering*. Tata McGraw-Hill, New York.

[32] Phadke, M. S. (1989) *Quality Engineering Using Robust Design*. Prentice-Hall, Englewood Cliffs, NJ.

[33] Song, Q., Shepperd, M., & Mair, C. (2005, September). Using grey relational analysis to predict software effort with small data sets. *11th IEEE International Software Metrics Symposium (METRICS'05)*, 10. https://doi.org/10.1109/METRICS.2005.51

[34] Visagan, A., Ganesh P. (2022). Parametric Optimization of Two Point Incremental Forming Using GRA and TOPSIS. *International Journal of Simulation Modelling, 21*(4), 615-626. https://doi.org/10.2507/IJSIMM21-4-622

[35] Yang, W.M., Li, C.D., Chen, Y.H., & Yu, Y.Y. (2021). Change impact analysis of complex product using an improved three-parameter interval grey relation model. *Advances in Production Engineering & Management, 16*(2), 185-198. https://doi.org/10.14743/apem2021.2.393

[36] Sallehuddin, R., Shamsuddin, S. M., & Hashim, S. Z. M. (2010, March). Forecasting small data set using hybrid cooperative feature selection. *2010 12th International Conference on Computer Modelling and Simulation*, 80-85. https://doi.org/10.1109/UKSIM.2010.23

[37] Fan, W., Xu, Z., Wu, B., He, Y., & Zhang, Z. (2022). Structural multi-objective topology optimization and application based on the criteria importance through intercriteria correlation method. *Engineering optimization, 54*(5), 830-846. https://doi.org/10.1080/0305215X.2021.1901087

[38] Banerjee, S., Mondal, S., Chatterjee, P., & Pramanick, A. K. (2021). An intercriteria correlation model for sustainable automotive body material selection. *Journal of Industrial Engineering and Decision Making*, *2*(1), 8-14. https://doi.org/10.31181/jiedm200201008b

[39] Keshavarz Ghorabaee, M., Amiri, M., Kazimieras Zavadskas, E., & Antuchevičienė, J. (2017). Assessment of third-party logistics providers using a CRITIC-WASPAS approach with interval type-2 fuzzy sets. *Transport*, *32*(1), 66-78. https://doi.org/10.3846/16484142.2017.1282381

[40] Mishra, P. S. & Muhuri, S. (2021). Value assessment of existing architectural heritage for future generation using criteria importance through inter-criteria correlation and grey relational analysis method: A case of Odisha temple architecture in India. *Current Science*, *121*(6), 823-833. https://doi.org/10.18520/cs/v121/i6/823-833

Contact information:

Ritesh Kumar SINGH, Associate Professor
Department of Production and Industrial Engineering,
Birla Institute of Technology, Mesra - Ranchi,
Jharkhand, India - 835215
E-mail: riteshsingh@bitmesra.ac.in

Sanjiv Kumar TIWARI, Assistant Professor
(Corresponding author)
Department of Production and Industrial Engineering,
Birla Institute of Technology, Mesra - Ranchi,
Jharkhand, India - 835215
E-mail: sanjivtiwari@bitmesra.ac.in

Sharad Chandra SRIVASTAVA, Professor
Department of Industrial and Production Engineering,
Guru Ghasidas Vishwavidyalaya, Bilaspur (A Central University),
Chhattisgarh, India - 495009
E-mail: sharadscs2@gmail.com

Binay KUMAR, Assistant Professor
Department of Production and Industrial Engineering,
Birla Institute of Technology, Mesra - Ranchi,
Jharkhand, India - 835215
E-mail: binaykumar@bitmesra.ac.in